

Shape from Silhouettes III

Guido Gerig

CS 6643, Spring 2017

(credit: slides modified from Marc Pollefeys

UNC Chapel Hill, some of the figures and slides are adapted from M. Pollefeys, J.S. Franco, J. Matusik's presentations, and referenced papers)



Outline

- Silhouettes
 - basic concepts
 - extract silhouettes
 - fundamentals about using silhouettes
 - reconstruct shapes from silhouettes
 - use uncertain silhouettes
 - calibrate from silhouettes
- Perspectives and cool ideas

Silhouette Consistency Constraints: Forbes et al.

- <http://www.dip.ee.uct.ac.za/~kforbes/Publications/Publications.html>
- Keith Forbes, Anthon Voigt and Ndimi Bodika. [Using Silhouette Consistency Constraints to Build 3D Models](#). In *Proceedings of the Fourteenth Annual Symposium of the Pattern Recognition Association of South Africa (PRASA 2003)*, November 2003.
- Keith Forbes, Anthon Voigt and Ndimi Bodika. [Visual Hulls from Single Uncalibrated Snapshots Using Two Planar Mirrors](#). In *Proceedings of the Fifteenth Annual Symposium of the Pattern Recognition Association of South Africa (PRASA 2004)*, November 2004.



Merging sets of silhouettes (Forbes et al.)

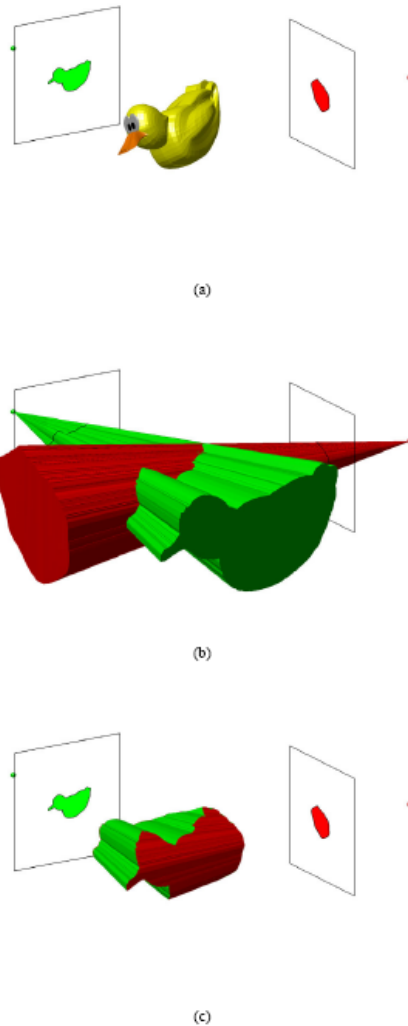


Figure 1: Two silhouette views of a duck showing (a) the cameras, each represented by a camera centre and image plane, (b) the visual cones corresponding to each of the two silhouettes, and (c) the visual hull corresponding to the two silhouettes.

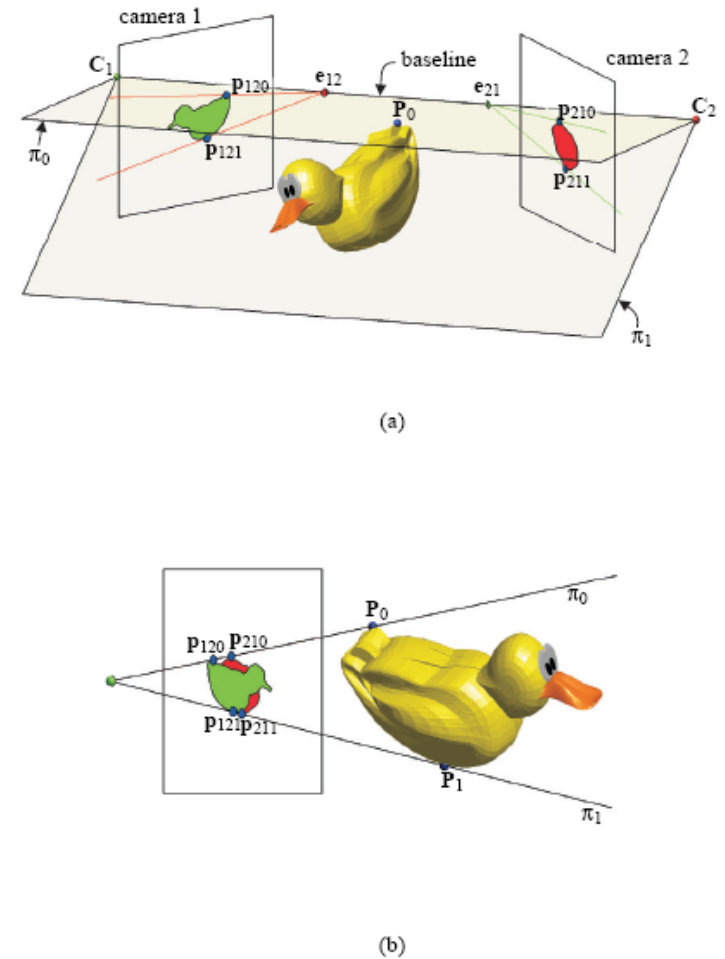


Figure 2: Two views of the epipolar geometry of a scene: (a) shows a front view, and (b) shows a side view looking onto the scene in a direction parallel to the baseline.

Review Epipolar Geometry Matrix Form



$$\mathbf{p} \cdot [\mathbf{t} \times (\mathcal{R}\mathbf{p}')] = 0$$

$$\vec{a} \times \vec{b} = [a_x] \vec{b}$$

$$\mathbf{p}^T [t_x] \mathcal{R} \mathbf{p}' = 0$$

$$\mathcal{E} = [t_x] \mathcal{R}$$

$$\mathbf{p}^T \mathcal{E} \mathbf{p}' = 0$$



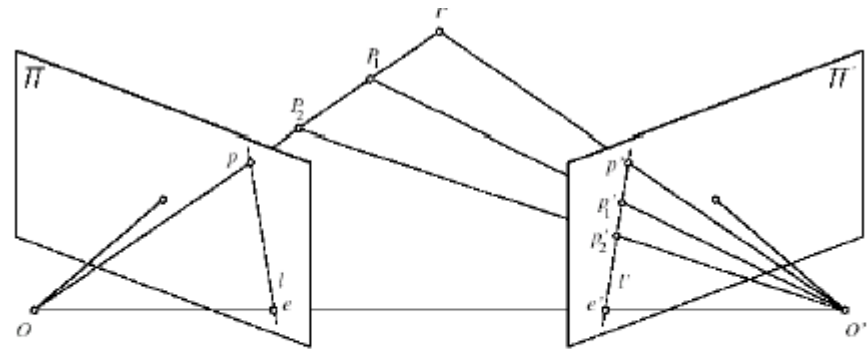
Review Epipolar Geometry

The Essential Matrix

Matrix that relates image of point in one camera to a second camera, given translation and rotation.

$$\mathcal{E} = [t_x] \mathfrak{R}$$

$$p^T \mathcal{E} p' = 0$$



$$\vec{a} \times \vec{b} = [a_x] \vec{b}$$

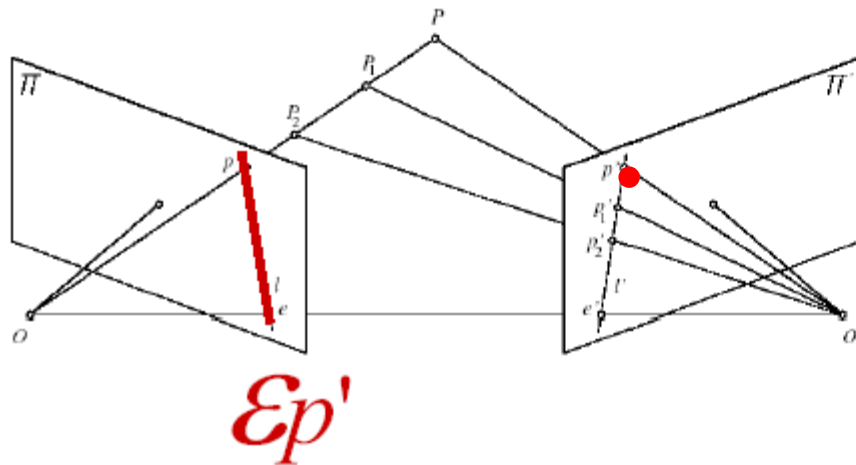


Review Epipolar Geometry

The Essential Matrix

$\mathcal{E}p'$ is the epipolar line corresponding to p' in the left camera.

$$au + bv + c = 0$$



$$p = (u, v, 1)^T$$

$$l = (a, b, c)^T$$

$$l \cdot p = 0$$

$$\mathcal{E}p' \cdot p = 0$$

$$p^T \mathcal{E}p' = 0$$

Similarly $\mathcal{E}p$ is the epipolar line corresponding to p in the right camera

Merging sets of silhouettes (Forbes et al.)

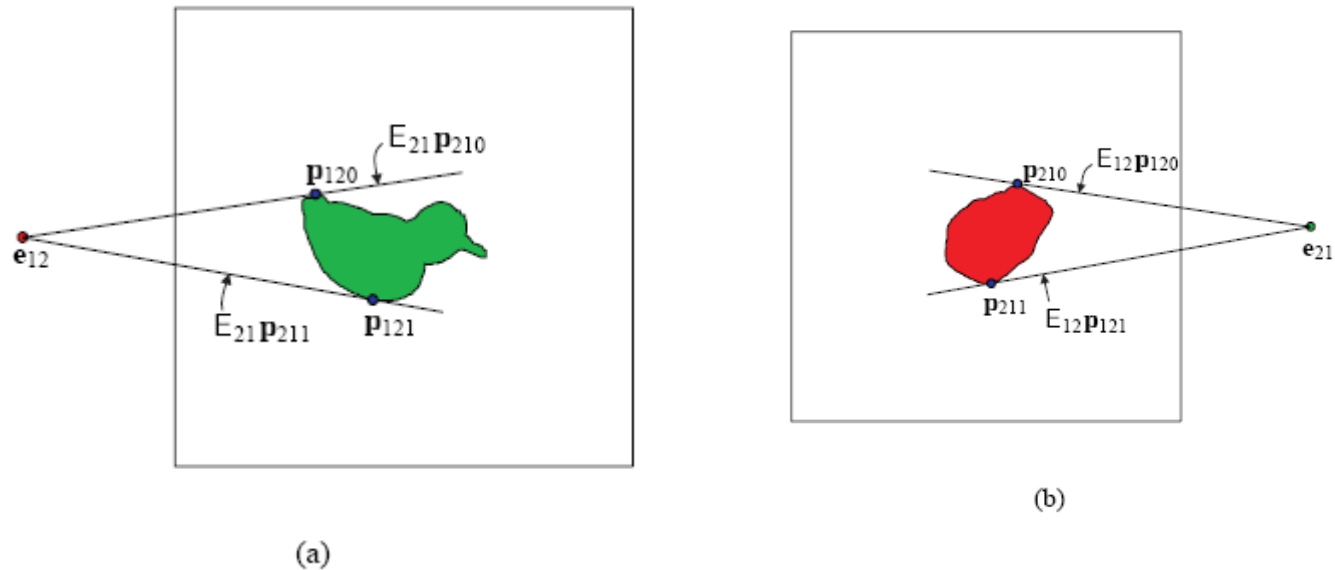
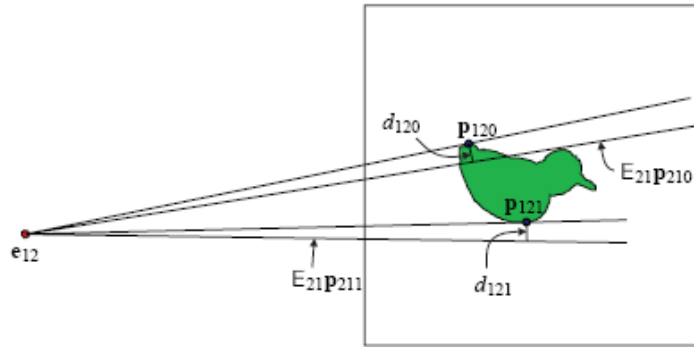


Figure 3: The epipolar tangency constraint: the epipolar tangent line touches the silhouette at the projection of the frontier point, as shown in (a) and (b); the projection of this line onto the image plane of the opposite camera is constrained to coincide with the opposite epipolar tangency line.

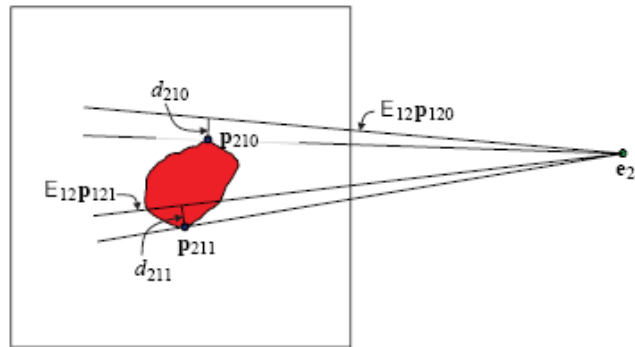
- $\mathbf{P}_0, \mathbf{P}_1$: Frontier points
- $\mathbf{p}_{120}, \mathbf{p}_{210}$ projections of \mathbf{P}_0 ($\mathbf{p}_{121}, \mathbf{p}_{211} \rightarrow \mathbf{P}_1$)
- Epipolar geometry: line $\mathbf{e}_{12}\mathbf{p}_{120}$ same as line defined by $E_{21}\mathbf{p}_{210}$



Reprojection Errors: Measure of Inconsistencies



(a)



(b)

- Reprojection error: Shortest distance from epipolar tangency to epipolar line of corresponding point
- Distances can be computed via $E_{ij} \rightarrow$ cost function associated to pose

$$d_{ijk} = \frac{\mathbf{p}_{ijk}^T \mathbf{E}_{ij} \mathbf{p}_{jik}}{\sqrt{(\mathbf{E}_{ij} \mathbf{p}_{jik})_1^2 + (\mathbf{E}_{ij} \mathbf{p}_{jik})_2^2}}$$

- **Pose estimation:** Adjust pose parameters to minimize cost fct:

$$\text{cost} = \sum_{i=1}^m \sum_{j=1}^n \sum_{k=0}^1 d_{ijk}^2$$

Figure 4: Epipolar tangent lines with the projection of the epipolar tangent line of the opposite view and incorrect pose information: since the pose information is incorrect, the epipolar tangent lines do not project onto one another. The silhouettes are inconsistent with one another for the given viewpoints. The reprojection error is a measure of the degree of inconsistency.

Results

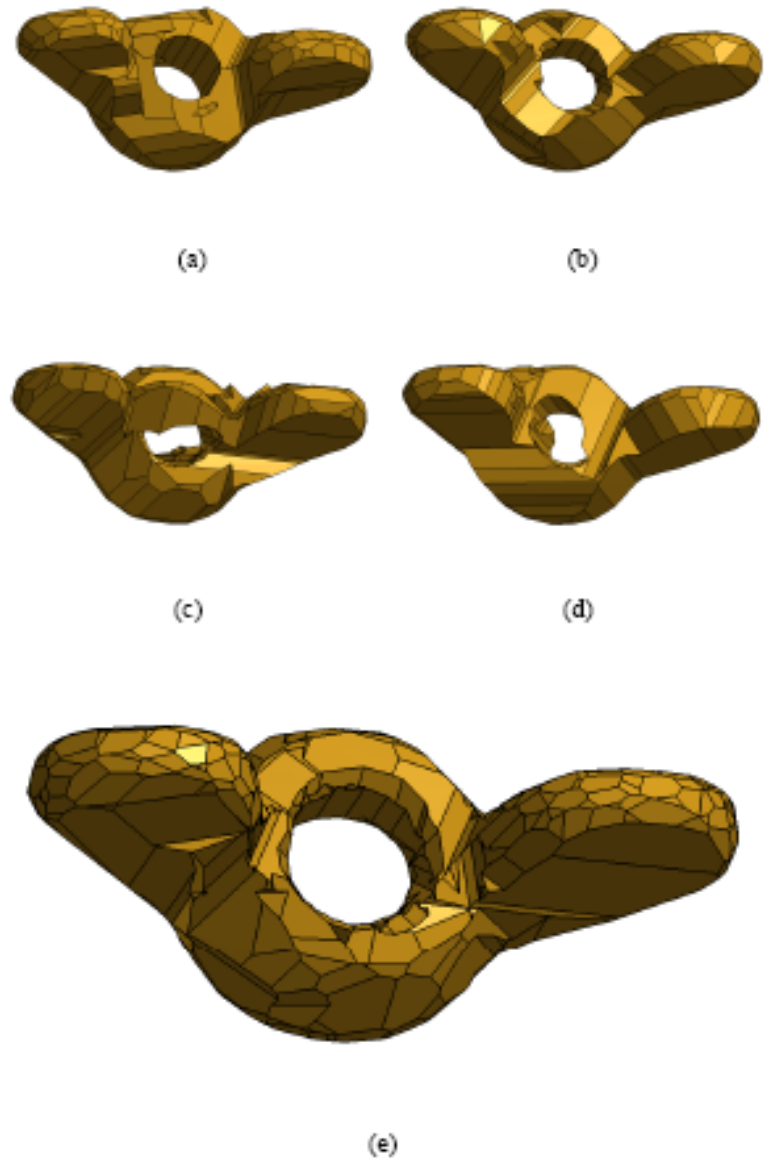


Figure 5: Visual hull models of a wing nut: (a)–(d) show four models each built from five silhouettes, (e) shows the model built from the 20 silhouettes used in (a)–(d) after the poses of all silhouettes have been determined in a common reference frame.

Results

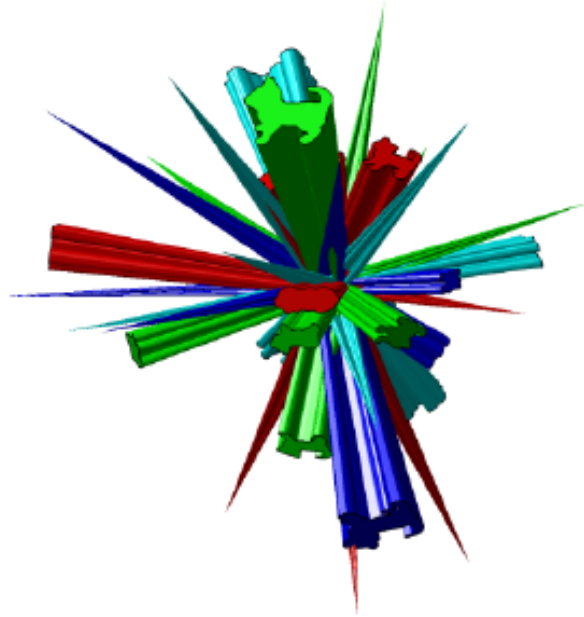
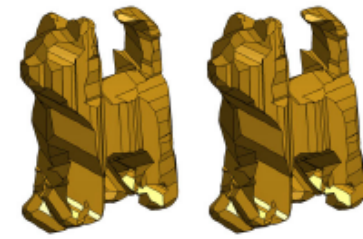


Figure 7: The twenty visual cones of the cat



(a)

(b)



(c)

(d)



(e)

Figure 6: Visual hull models of a toy cat: (a)–(d) show four models each built from five silhouettes, (e) shows the model built from the 20 silhouettes used in (a)–(d) after the poses of all silhouettes have been determined in a common reference frame.

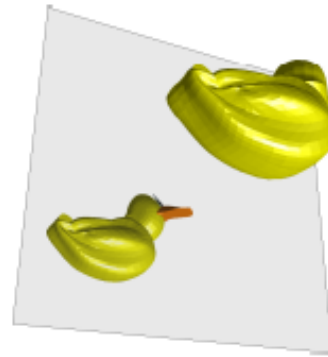
Smart Low Cost Solution

- **Visual Hulls from Single Uncalibrated Snapshots Using Two Planar Mirrors**
- Keith Forbes,
Anthon Voigt,
Ndimi Bodika,
PRASA2004 ([link](#))

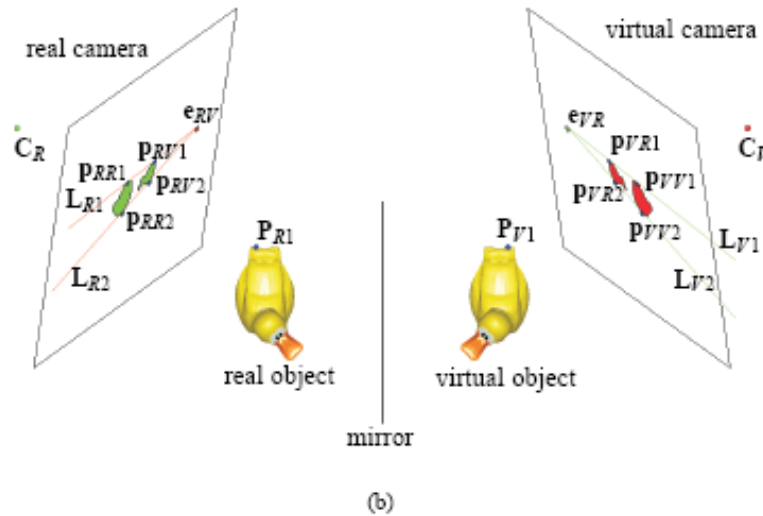




Concept



(a)



(b)

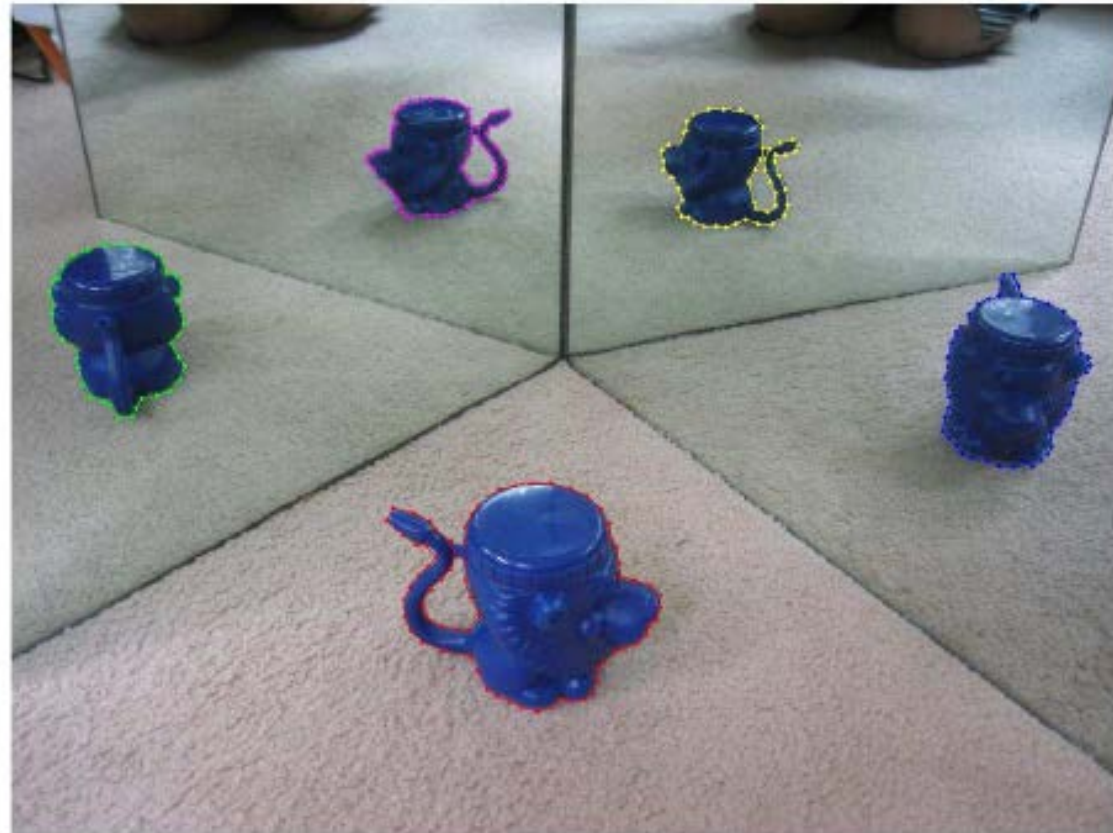
- Virtual camera does not really exist
- Determine images it would observe from the real camera's image
- Therefore: Two silhouettes captured by real camera are **two views of the real object**

Figure 2: Reflection of a duck in a mirror: (a) shows the image seen by the real camera, (b) shows the silhouette views seen by the real camera and by the virtual camera that is the reflection of the real camera.



Visual Hulls from 2 Mirrors

Then I manually segmented the five silhouettes in Matlab using polygons. The coordinates of the five polygons are the inputs to the Matlab code used to calculate the visual hull.

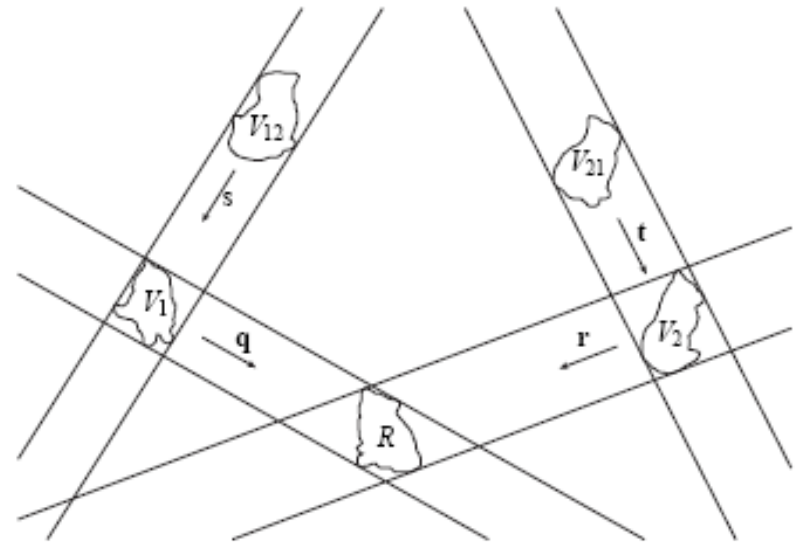


Visual Hulls from 2 Mirrors



- Epipolar geometry of the object's five silhouettes is determined directly from the image without knowing the poses of the camera or the mirrors.
- Once the pose associated with each silhouette has been computed, a five-view visual hull of the object can be computed from the five silhouettes.
- After getting an initial estimation of all the camera poses, we can use the non-linear least square Levenberg-Marquardt method to iteratively minimize the reprojection error across every pair of silhouettes.

Similar as before: Epipolar Tangency Lines



(c)

Figure 4: Images of a scene: (a) shows the raw image, (b) shows the segmented image with silhouette outlines and epipolar tangency lines, and (c) shows the derived orthographic image that would be seen by an orthographic camera.

Visual Hulls from 2 Mirrors

(Forbes et al.)

Figure 4.5 shows how the epipoles e_{V1} , e_{V2} , e_{V121} , and e_{V212} are computed from the outlines of the five silhouettes observed by the real camera.

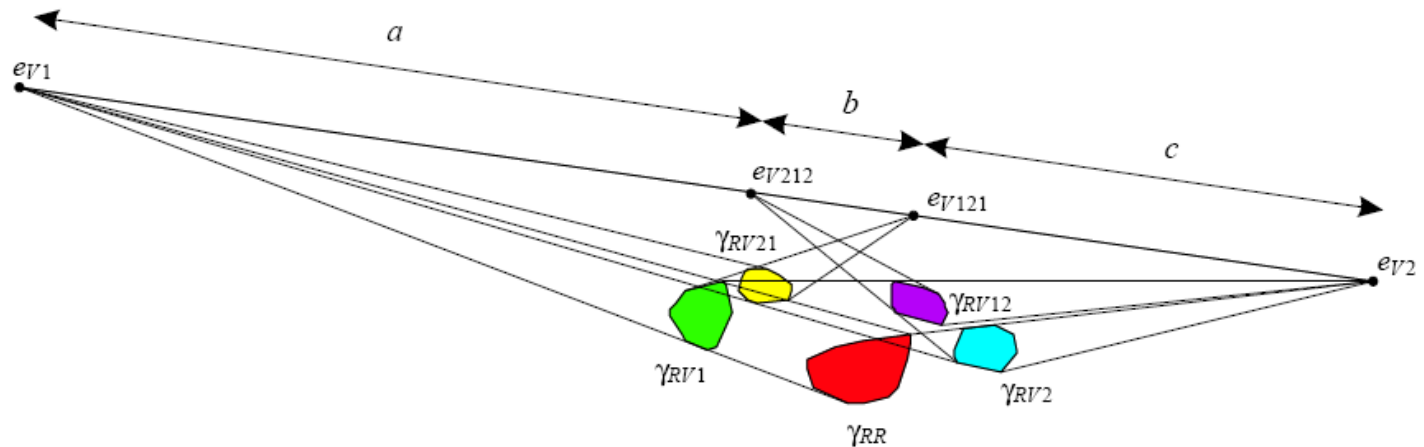
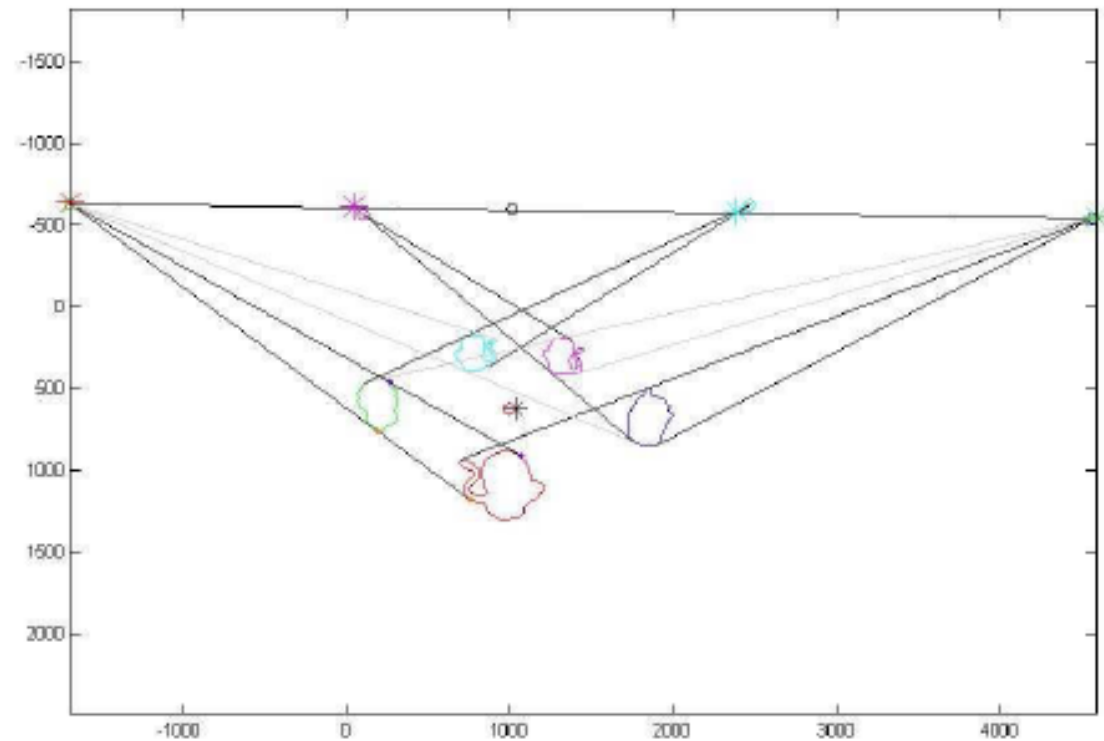


Figure 4.5: Computing epipoles e_{V1} , e_{V2} , e_{V121} , and e_{V212} from the silhouette outlines in an image.

Note that the epipoles e_{V1} , e_{V2} , e_{V121} , and e_{V212} are collinear, since they all lie in both the image plane of the real camera and in the plane PC in which all camera centres lie.

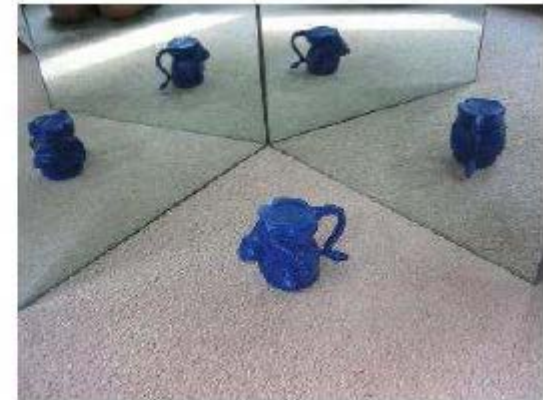
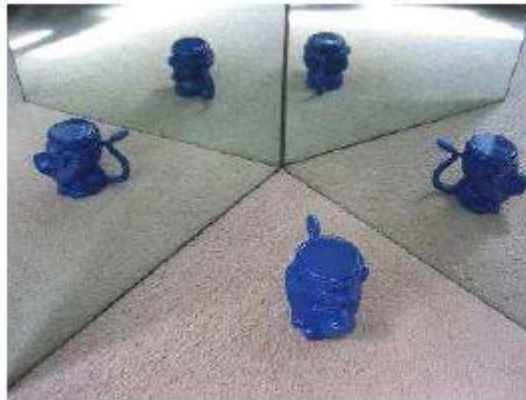
Visual Hulls from 2 Mirrors

The four colinear epipoles determined directly using silhouette outlines are showed as follows.





Visual Hulls from 2 Mirrors: Merge multiple 5 view hulls

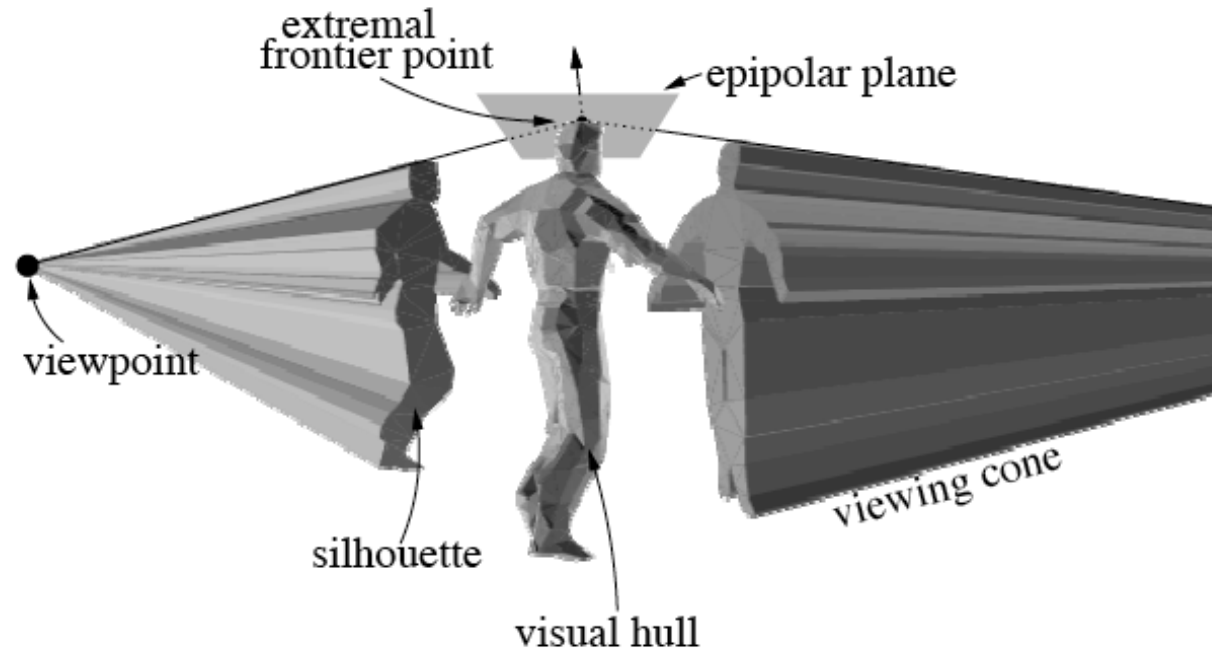


Christine Xu: Calculations in Matlab, all calculations <1Min

What if my views aren't calibrated at all?

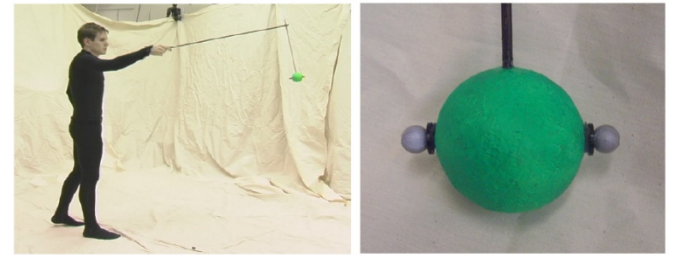
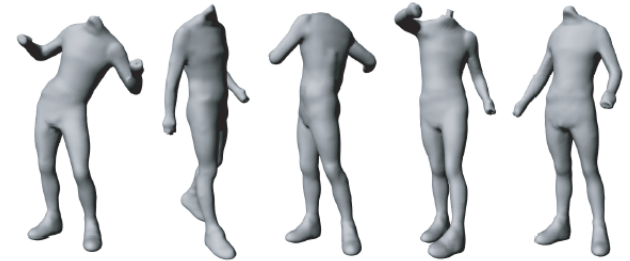


- Possible to calibrate from silhouettes
- Idea: optimize for a set of calibration parameters most consistent with silhouettes
- Boyer 05: define a dense distance between two cones
 - minimize the combined distances between viewing cones





Camera network calibration using silhouettes



- 4 NTSC videos recorded by 4 computers for 4 minutes
- Manually synchronized and calibrated using MoCap system

Additional slides:
Not used in Class

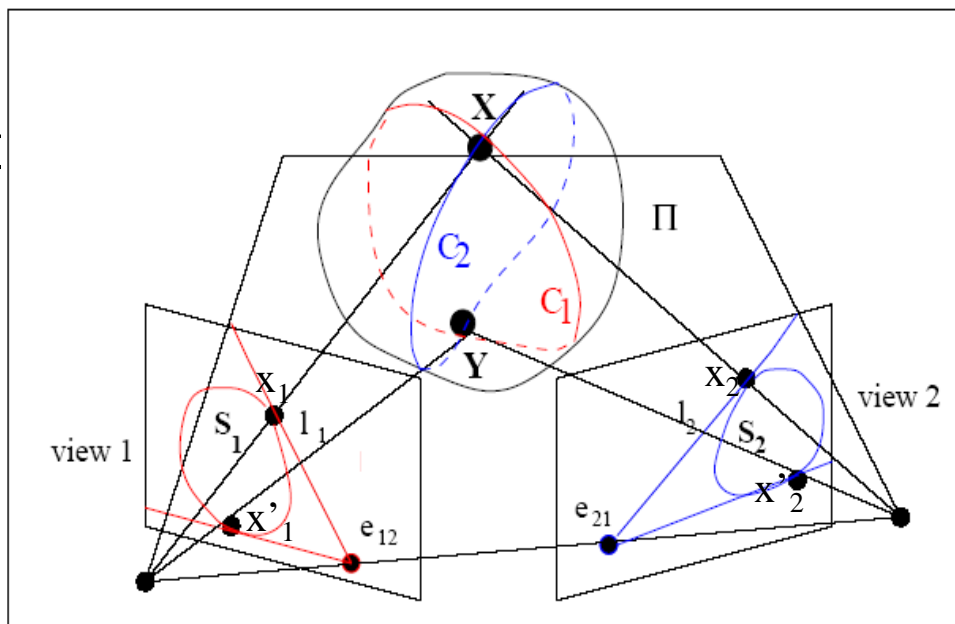


Multiple View Geometry of Silhouettes

- Frontier Points
- Epipolar Tangent

$$\mathbf{x}_2^T \mathbf{F} \mathbf{x}_1 = 0$$

$$\mathbf{x}'_2{}^T \mathbf{F} \mathbf{x}'_1 = 0$$



- Points on Silhouettes in 2 views do not correspond in general except for projected Frontier Points
- Always at least 2 extremal frontier points per silhouette
- In general, correspondence only over two views

Camera Network Calibration from Silhouettes

(Sinha et al, CVPR'04)

- 7 or more corresponding frontier points needed to compute epipolar geometry for general motion
- Hard to find on single silhouette and possibly occluded

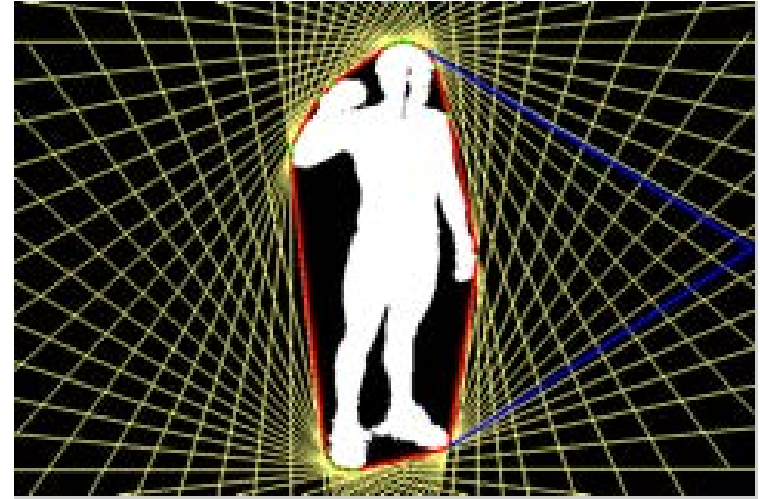


However, Visual Hull systems record many silhouettes!

A Compact Representation for Silhouettes

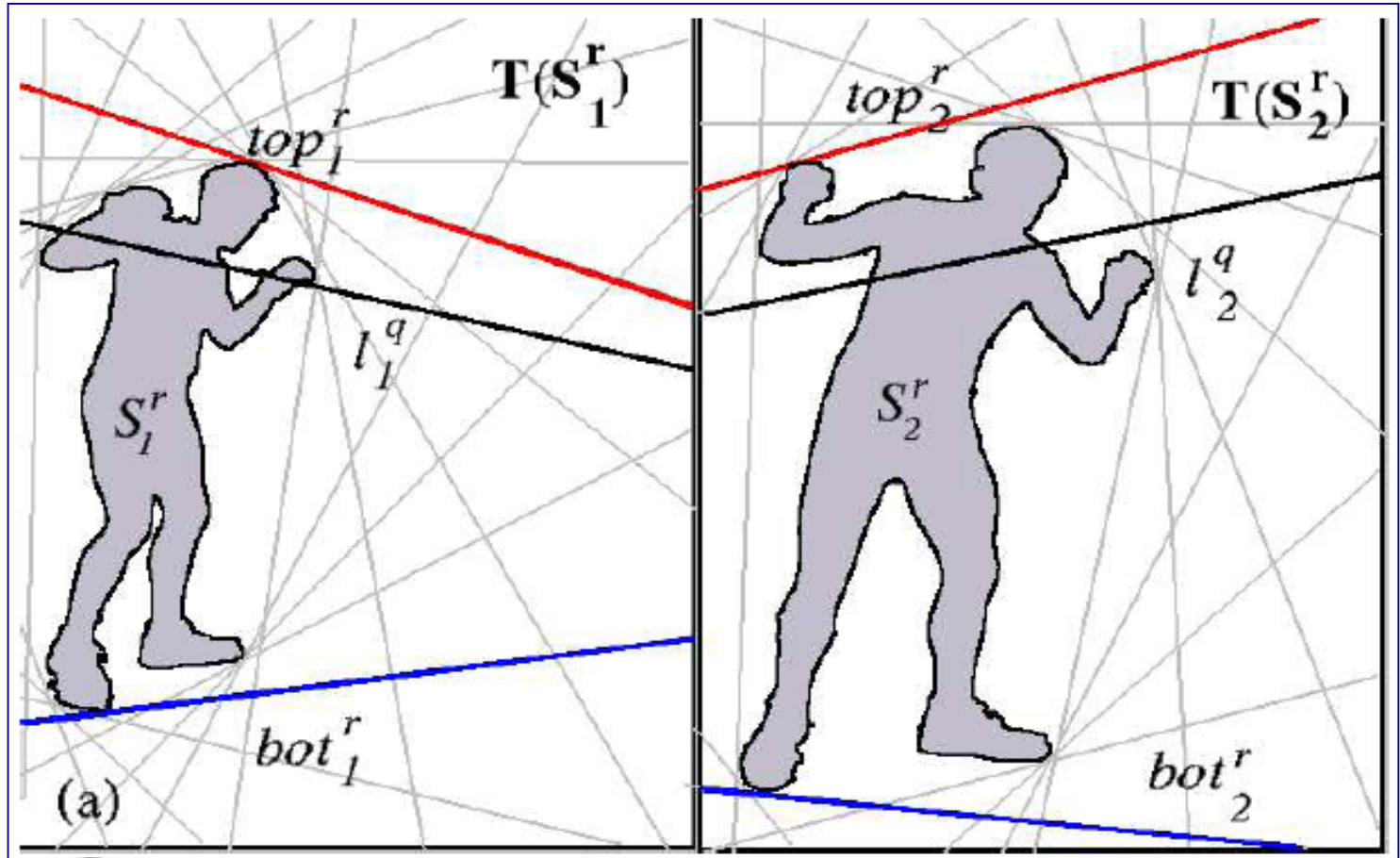
Tangent Envelopes

- Convex Hull of Silhouette.
- Tangency Points for a discrete set of angles.



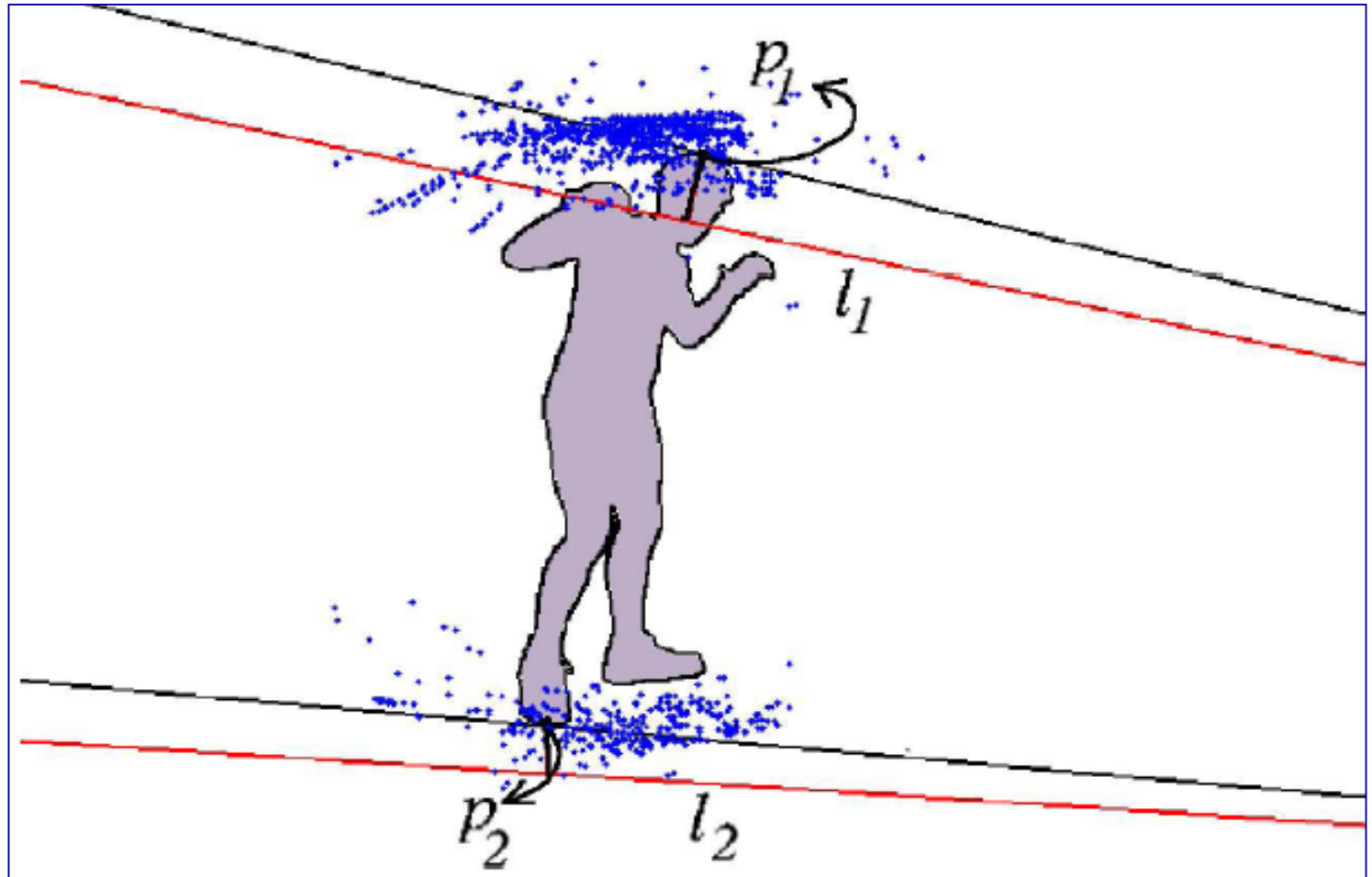
- Approx. 500 bytes/frame. Hence a whole video sequences easily fits in memory.
- Tangency Computations are efficient.

Epipole Hypothesis and Computing H





Model Verification





Why use a Visual Hull?

- Can be computed efficiently
- No photo-consistency required
- As bootstrap of many fancy refinement ...

Why not a Visual Hull?

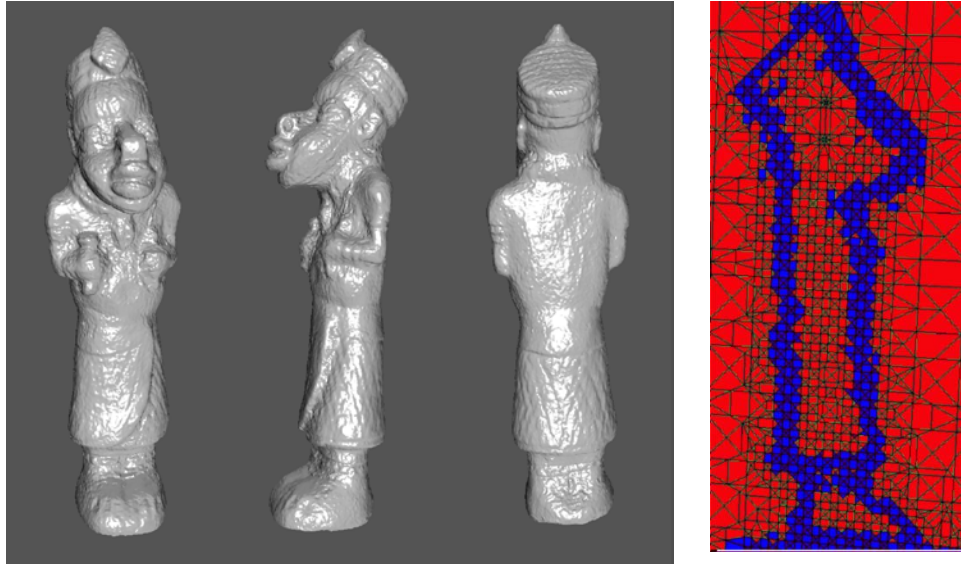
- No exact representation in concavity
- Sensitive to silhouette observation
- Closed surface representation
- Silhouette loses some information ...



Literature

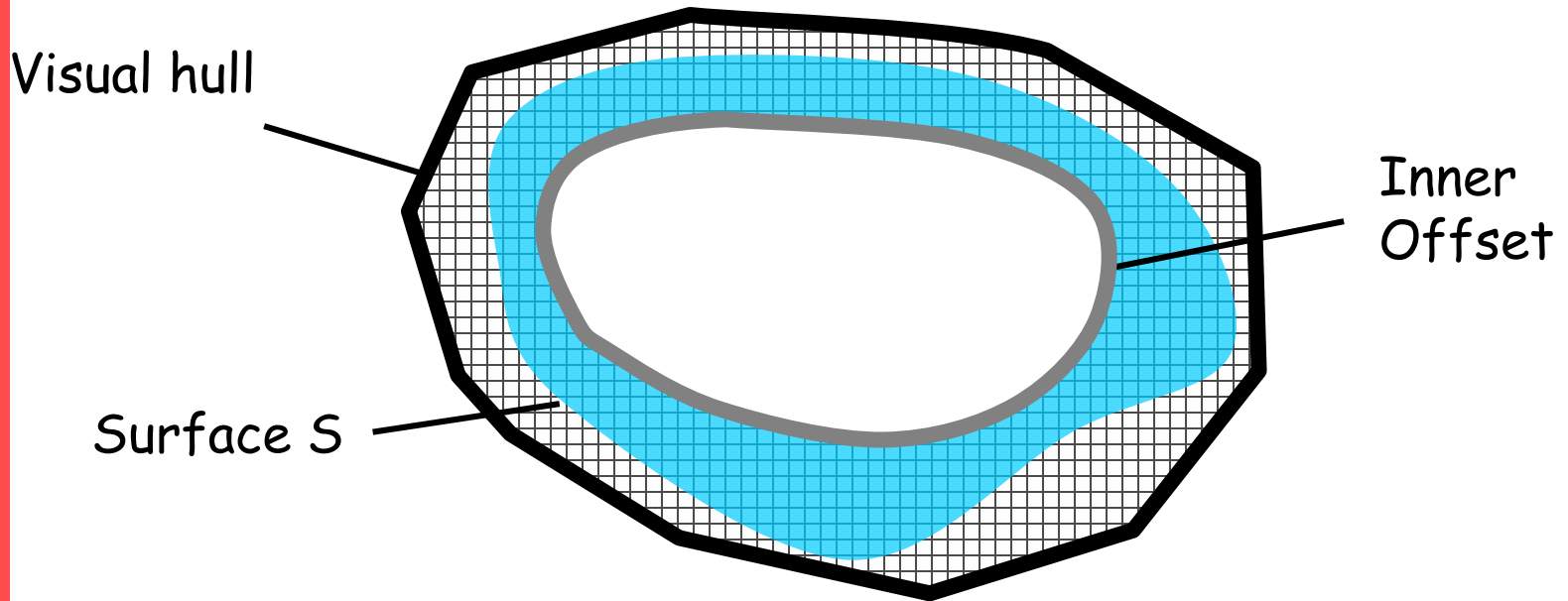
- Theory
 - Laurentini '94, Petitjean '98, Laurentini '99
- Solid cone intersection:
 - Baumgart '74 (polyhedra), Szeliski '93 (octrees)
- Image-based visual hulls
 - Matusik et al. '00, Matusik et al. '01
- Advanced modeling
 - Sullivan & Ponce '98, Cross & Zisserman '00, Matusik et al. '02
- Applications
 - Leibe et al. '00, Lok '01, Shlyakhter et al. '01, ...

Extension: Multi-view Stereo with exact silhouette constraints



Sinha Sudipta, PhD thesis UNC 2008,
**Silhouettes for Calibration and
Reconstruction from Multiple Views**

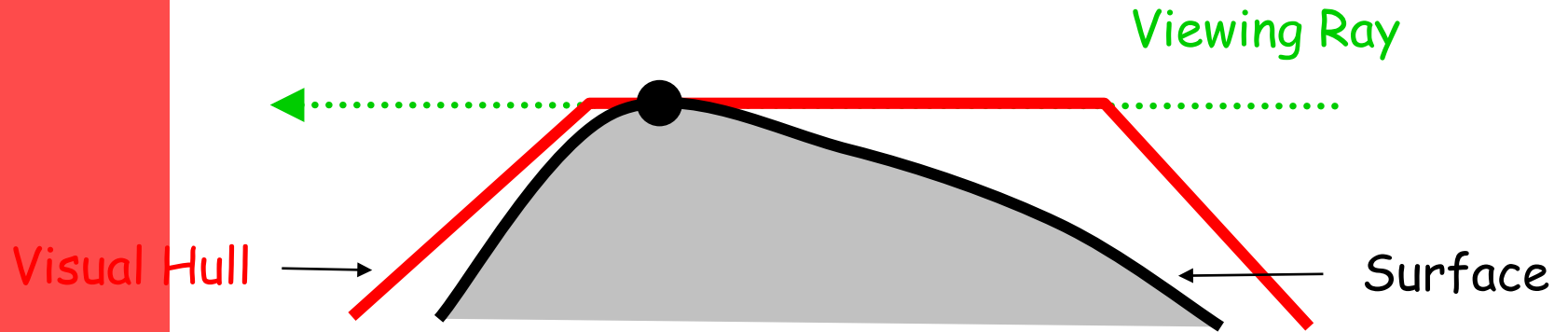
Volumetric Formulation



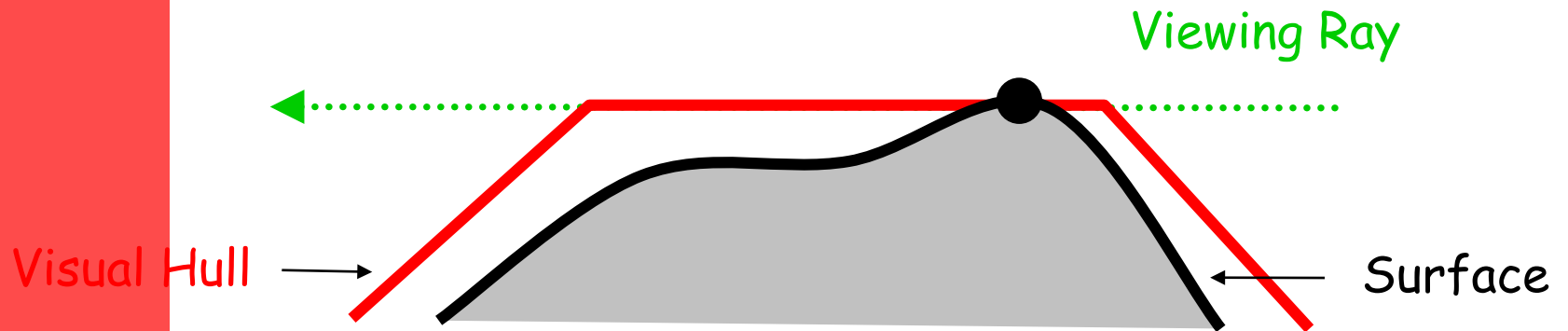
Find S which minimizes $\int_S \phi(s) ds$

$\phi(s)$ is a measure of the photo-inconsistency of a surface element at s

Silhouette Consistent Shapes



Silhouette Consistent Shapes





Photoconsistency

- **Photo-consistency** is a function that how measures the likelihood of a 3D point of being on a opaque surface in the scene. This likelihood is computed based on the images in which this 3D point is potentially visible.
- An ideal Lambertian surface point will appear to have the **same color in all the images**.
- Photo-consistency can be measured in image space or object space.
 - Image space computations compare image patches centered at the pixels where the 3D point projects.
 - Object space computations are more general – a patch centered at the 3D point is projected into the images and the appearance of the projected patches are compared.

Photoconsistency

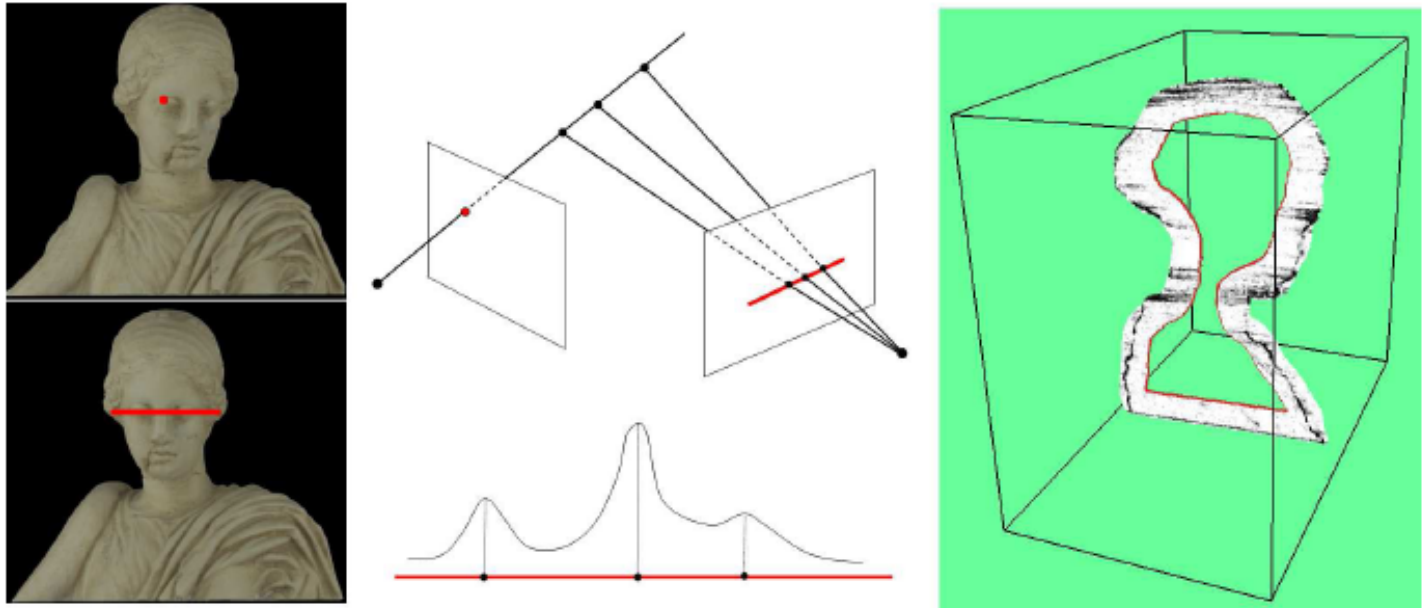
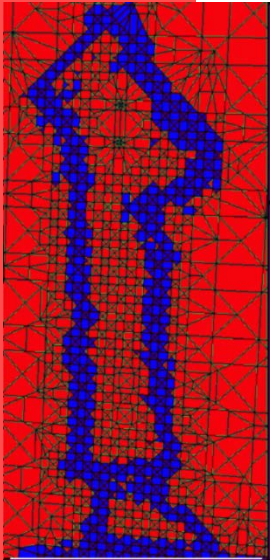


Figure 6.19: Computing multiple hypotheses for 2-view matches. These 2-view matches are triangulated and the generated 3D points are used to accumulate votes within a 3D volume. The photo-consistency measure is derived from these votes. A slice through the photo-consistency volume (interior of visual hull) is shown. Here black indicates regions of high photo-consistency.

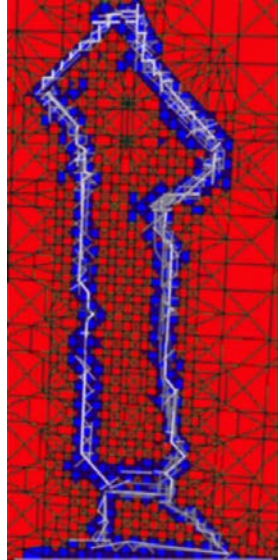
Sinha Sudipta, PhD thesis UNC 2008,
**Silhouettes for Calibration and
Reconstruction from Multiple Views**



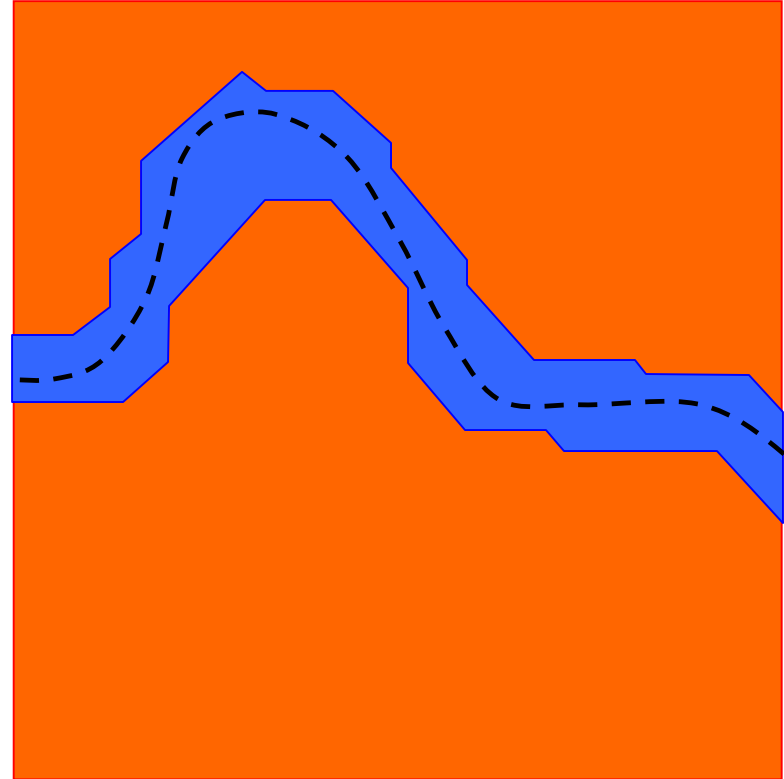
Mesh with Photo-consistency



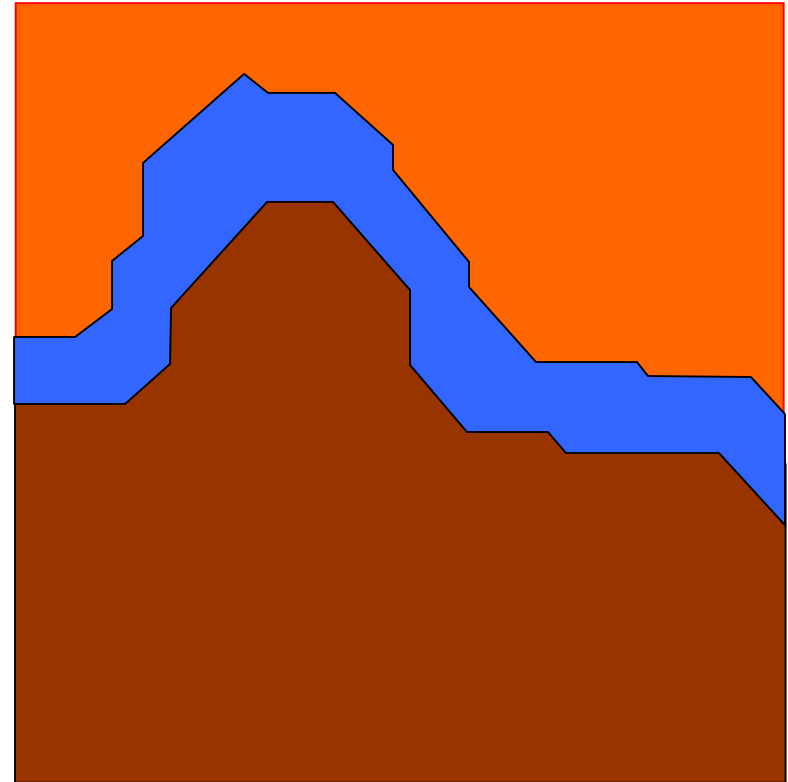
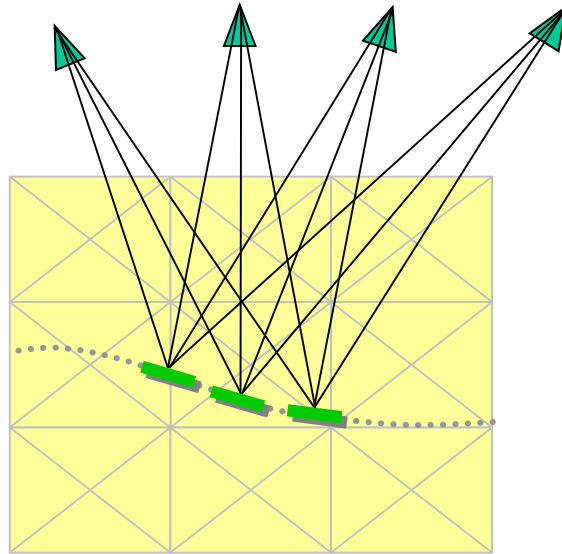
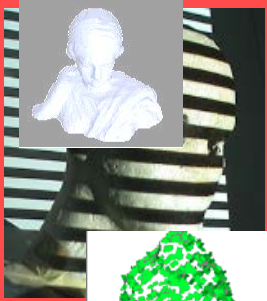
Final Mesh



shown with
Photo-consistency



Detect Interior



Use Visibility of the
Photo-consistent Patches

Also proposed by
Hernandez et. al. 2007, Labatut et.

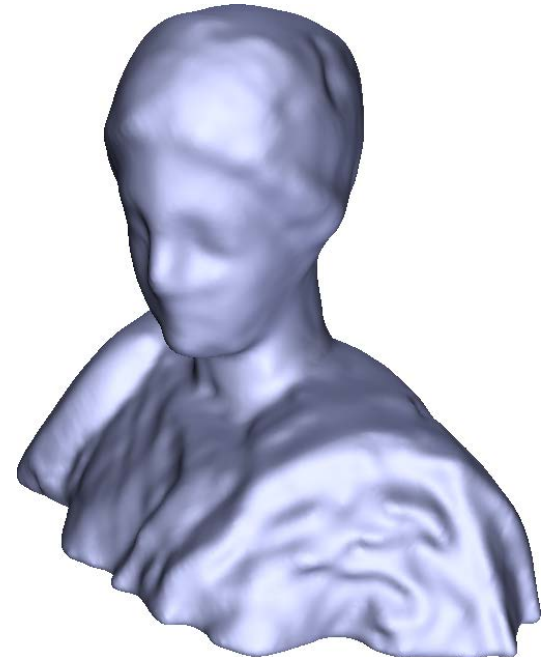
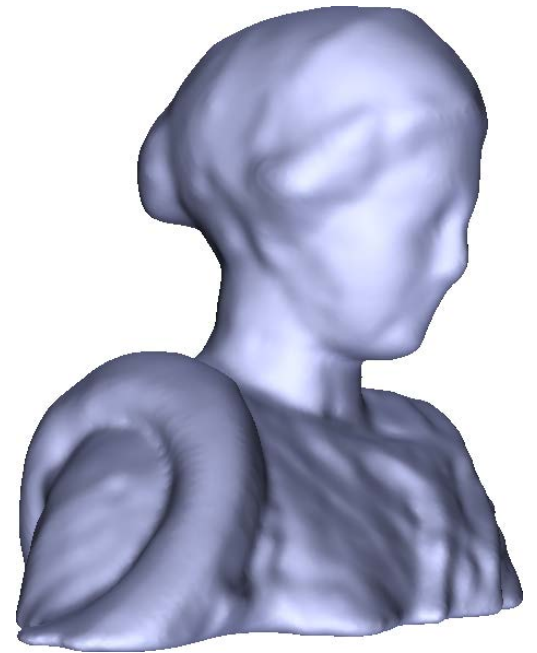
Results



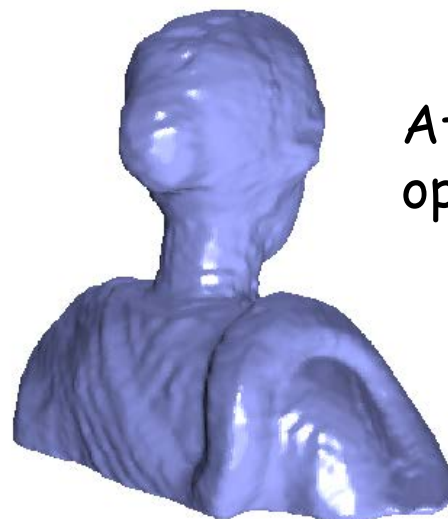
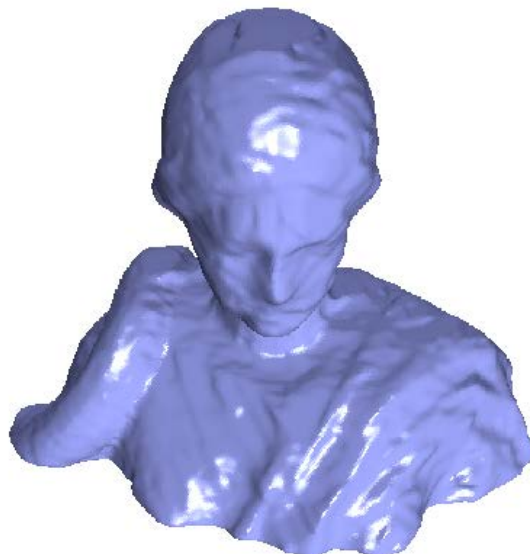
**36
images**



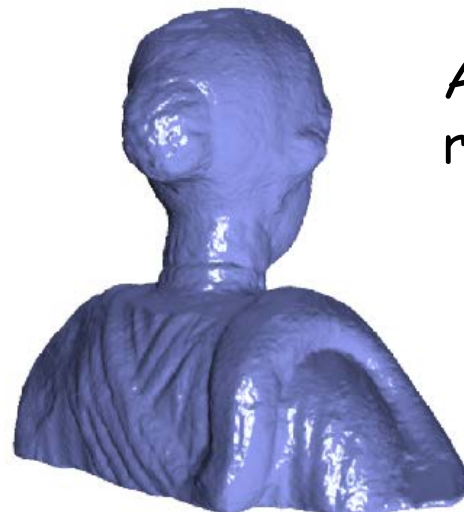
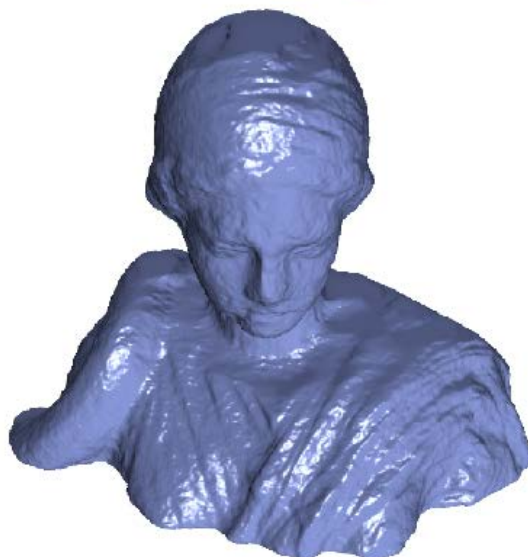
**36
images**



Results



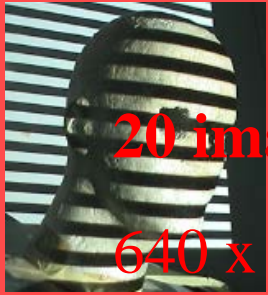
After graph-cut optimization



After local refinement

36
images

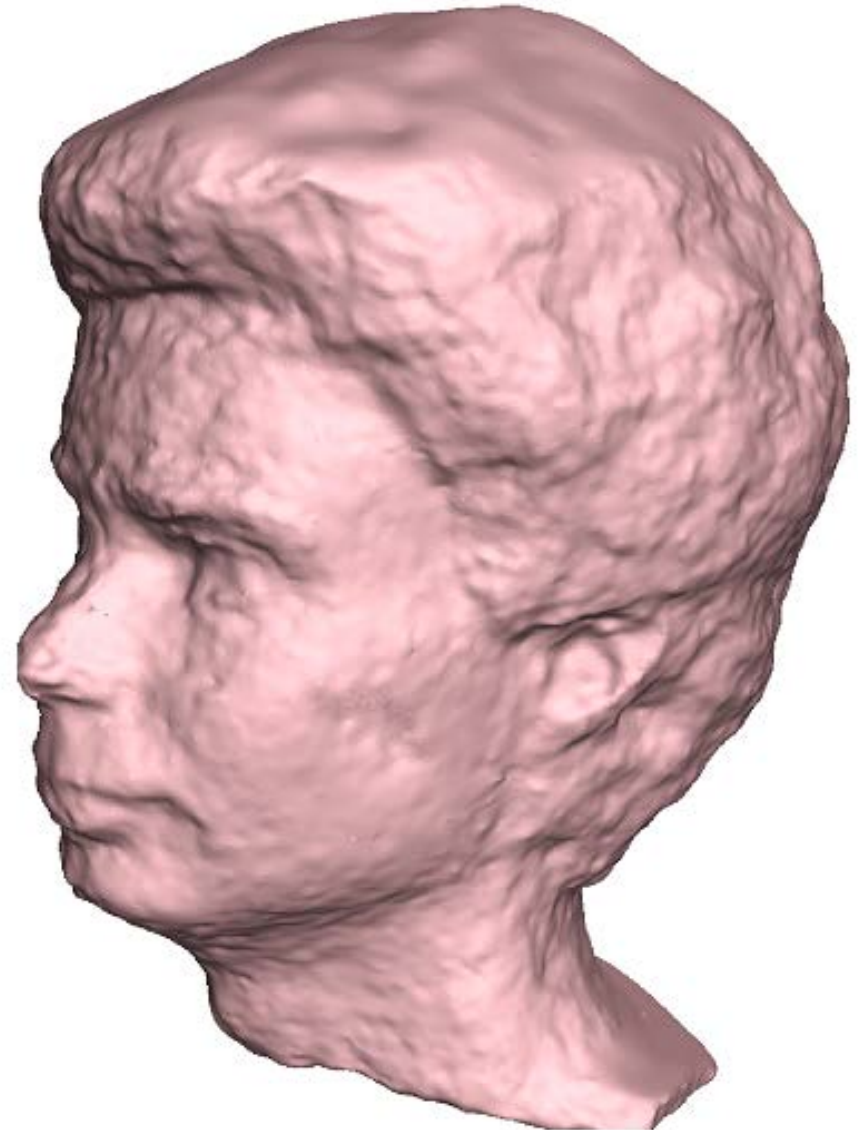
2000 x 3000



20 images

640 x 480

pixels

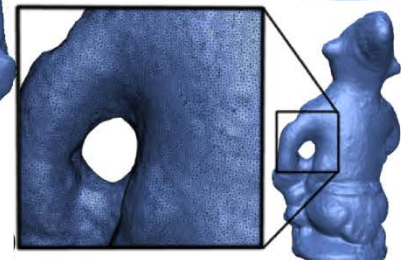
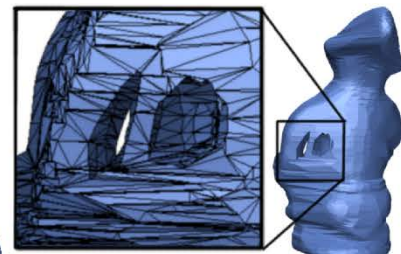


Running Time:

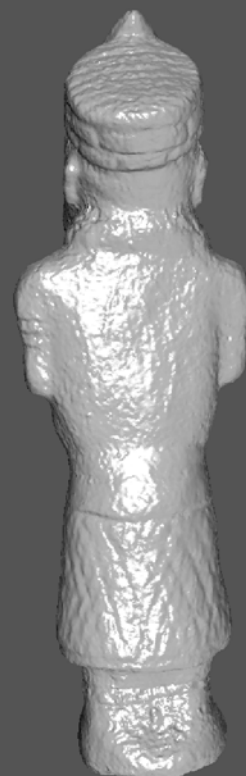
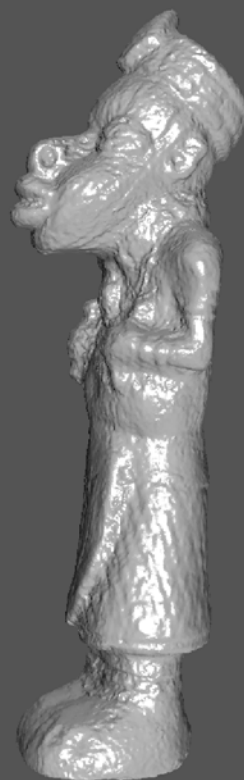
Graph Construction :
25 mins

Graph-cut :
5 mins

Local Refiner
20 mins



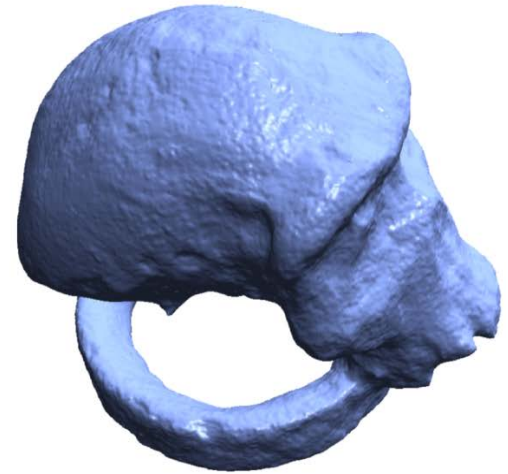
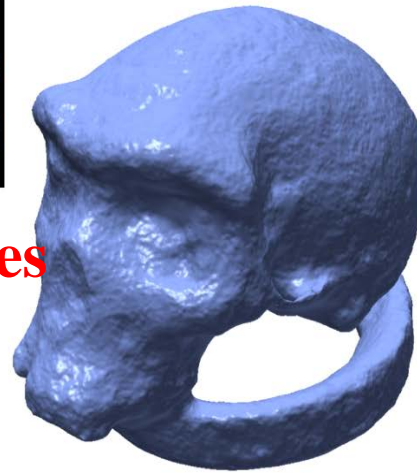
36
images



36
images



24 images

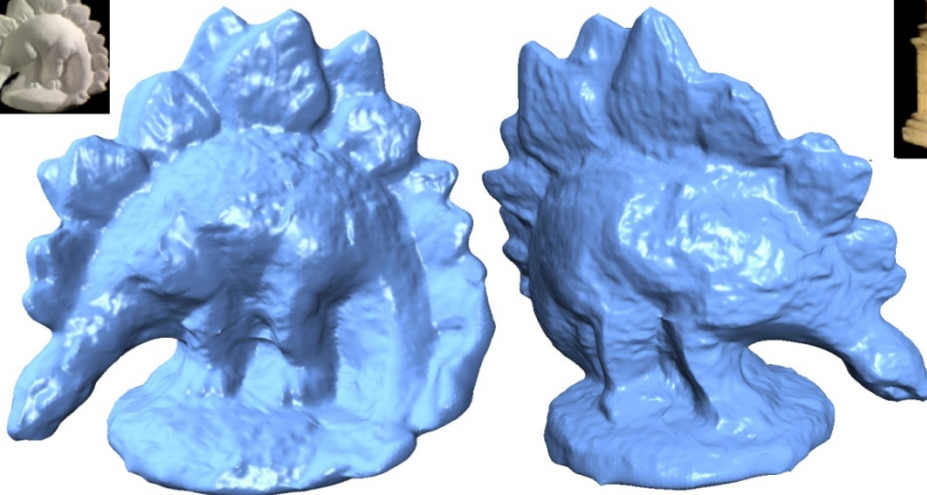


Middlebury Evaluation

90% statistics	Accuracy	Completeness		Time
Dino-ring	0.69 mm	97.2 %		110 mins.
Temple-ring	0.79 mm	94.9 %		104 mins.

48

ii



47

